Electronic structure of solid coronene: differences and commonalities to picene

Taichi Kosugi[1], Takashi Miyake[1,2], Shoji Ishibashi[1], Ryotaro Arita[2,3,4], and Hideo Aoki[5]

[1] *Nanosystem Research Institute "RICS", AIST, Umezono, Tsukuba 305-8568, Japan*

[2] *Japan Science and Technology Agency, CREST, Honcho, Kawaguchi, Saitama 332-0012, Japan*

[3] *Department of Applied Physics, University of Tokyo, Hongo, Tokyo 113-8656, Japan*

[4] *PRESTO, Japan Science and Technology Agency (JST), Kawaguchi, Saitama 332-0012, Japan and*

[5] *Department of Physics, University of Tokyo, Hongo, Tokyo 113-0033, Japan*

We have obtained the first-principles electronic structure of solid coronene, which has been recently discovered to exhibit superconductivity with potassium doping. Since coronene, along with picene, the first aromatic superconductor, now provide a class of superconductors as solids of aromatic compounds, here we compare the two cases in examining the electronic structures. In the undoped coronene crystal, where the molecules are arranged in a herringbone structure with two molecules in a unit cell, the conduction band above an insulating gap is found to comprise four bands, which basically originate from the lowest two unoccupied molecular orbitals (doubly-degenerate, reflecting the high symmetry of the molecular shape) in an isolated molecule but the bands are entangled as in solid picene. The Fermi surface for a candidate of the structure of $K_x$coronene with $x = 3$, for which superconductivity is found, comprises multiple sheets, as in doped picene but exhibiting a larger anisotropy with different topology.

Introduction — Discovery of superconductivity in solid picene doped with potassium atoms [1] is seminal and came as a surprise in that the picene, on top of the highest T_c among organic superconductors, belongs to *aromatic* compounds, the most typical, textbook class of organic materials. Then a natural question to ask is: can other aromatic compounds become superconducting as well? Before examining this question, let us first briefly summarize the known superconductors in carbon-based materials. First discovery goes back to 1965, when a graphite-intercalation compound (GIC), KC_8, was found to be a superconductor at 0.1 K [2], and the highest T_c among GIC's to date is 11.6 K in CaC_6[3]. Fullerene is another class, where potassium-doped fullerene, K_3C_{60}, has $T_c = 20$ K [4], followed by Cs_2RbC_{60} with $T_c = 33$ K [5], or 40 K in Cs_3C_{60} under 15 kbar [6]. In the last decade, the boron-doped diamond [7] joined carbon-based superconductors. The first aromatic superconductivity in the potassium-doped solid picene discovered by Kubozono's group[1], with $T_c = 7 - 18$ K in $K_x$picene for $x \simeq 3$, was unsuspected, since the (undoped) solid of picene (a hydrocarbon compound with five benzene rings connected in a zigzag) has been known to be a good insulator, as naturally expected for an aromatic molecule.

The present authors have reported for the first time the first-principles electronic structure of both undoped and doped solid picene in the framework of the density functional theory (DFT) within the local density approximation (LDA) [8]. We have revealed, first for the undoped solid picene, where picene molecules take a herringbone structure, that the conduction band consists of four bands, which originate basically from the lowest two unoccupied molecular orbitals (LUMO and LUMO+1) of an isolated molecule, but the bands are entangled (i.e., crossing with each other. When doped with potassium atoms, the herringbone structure is deformed, and

the electronic wave function significantly spills from the organic molecules' LUMO's into potassium sites[8].

Now, if we come back to the question of whether and which other aromatic compounds can become superconducting, recently Kubozono's group reported superconductivity in doped coronene [9]. Coronene, $C_{24}H_{12}$, is another of typical aromatic molecules, with seven benzene rings assembled in a concentric disk. Superconductivity in $K_x$coronene is reported to appear around $x \simeq 3$ with T_c up to 15 K.[10] Motivated by this, here we have obtained the electronic structure of solid coronene, both undoped and doped. An obvious interest is the differences and commonalities between the crystal and electronic structures of solid coronene as compared with those of solid picene. This is precisely the purpose of the present work. The obtained results are analyzed with maximally-localized Wannier functions (WF's) [11], in terms of which we downfold the system into a tight-binding model and compare with those for picene.

We shall show that the conduction band of the undoped solid coronene comprises four bands, which basically originate from the two LUMO's (doubly-degenerate, reflecting the symmetry of the molecule higher than that of picene) in an isolated molecule, but the bands are entangled as in solid picene. The Fermi surface for a candidate of the structure of $K_x$coronene with $x = 3$, for which superconductivity is found, comprises multiple sheets, as in doped picene but exhibiting a more one-dimensional character with different anisotropy nad topology.

The present electronic structure will serve as a basis for discussing mechanisms of the superconductivity. Since some classes of organic superconductors are considered to have an electronic mechanism,[12] picene and coronene superconductors may possibly belong to them. There have been some theoretical studies[13, 14] that suggest that solid picene is a strongly correlated elec-

tron system. As for the electron-phonon coupling, on the other hand, Kato *et al.* estimated the phonon frequencies and the electron-phonon coupling for various hydrocarbon molecules[15]. For picene they found that the electron-phonon coupling can be as large as 0.2 eV. While it is generally difficult to quantitatively estimate T_c for a phonon mechanism due to the ambiguity in the Coulomb pseudopotential (μ^*), they concluded that $T_c \sim 10$ K may be expected. They also estimated the coupling for coronene to be about 0.1 eV. Subedi *et al.*[16] recently calculated the phonon spectrum and electron-phonon interaction for solid picene, and they found that the calculated electron-phonon coupling 0.1-0.2 eV is sufficiently strong to reproduce the experimental T_c of 18 K within the Migdal-Eliashberg theory.

First-principles bands — The calculation is based on DFT, where LDA in the Perdew-Zunger formula is adopted for the exchange-correlation energy functional.[17] We use the projector-augmented wave (PAW) method[18], implemented to the Quantum MAterials Simulator (QMAS) package.[19] The pseudo Bloch wave functions are expanded by plane waves up to an energy cutoff of 40 Ry with $4 \times 6 \times 4$ k-points.

As for the crystal structure, here we adopt the experimental lattice parameters of natural coronene (karpatite) reported by Echigo *et al.* [20] Natural coronene has a monoclinic (space group: $P2_1/a$) structure with $a = 16.094, b = 4.690$ and $c = 10.049$ Å, and $\beta = 110.79°$. We have also performed calculations adopting the lattice parameters of synthetic coronene [21], and have confirmed that the results are essentially unchanged from those for the natural coronene. The molecular solid has a herringbone arrangement of molecules as depicted in Fig. 1 with a unit cell containing two molecules (centered respectively at $(0, 0, 0)$ and $(1/2, 1/2, 0)$ as dictated by the symmetry). The lattice parameters are fixed at the experimental values, and the internal atomic positions are optimized. The angle between the planes of the inequivalent molecules in the optimized geometry is 95°, which agrees with the measured value. It was found that the point-group symmetry D_{6h} for an isolated coronene molecule is lowered to D_{2h} in the crystal.

Figure 2 displays the electronic band structure of coronene. We have an insulator with a band gap of 2.41 eV. The gap, which is naturally smaller than the HOMO-LUMO gap, calculated to be 2.90 eV, of an isolated coronene molecule, is indirect, with the valence band top located at Y in the Brillouin zone, while the conduction band bottom at Γ. Since the crystal structure is layered, where the herringbone arrangement, on the $a - b$ plane, of the molecules are stacked along c axis, the electronic structure is more dispersive along $a^* - b^*$ axis. More precisely, the dispersion along b^* is larger than that for a^*, which directly reflects the distance between neighboring molecules being shortest along b. The conduction band, with a width of 0.40 eV, consists of four bands derived from the doubly-degenerate, e_{1g} LUMO's. For solid picene by comparison, the conduction band, with a width of

0.39 eV, consists of four bands with a band gap of 2.36 eV, while the LUMO-HOMO gap of a picene molecule is 2.96 eV. These are similar to solid coronene, where a difference is the conduction band of the solid picene originates from LUMO and LUMO+1 of an isolated picene molecule [8]. Considering the general tendency of LDA to underestimate band gaps, we expect that the actual band gap of coronene may be larger than the calculated value. An accurate prediction of optical properties and band widths will also require incorporation of many-body effects, as is done with GW by Roth *et al.* [22] for picene. The valence band of solid coronene has a width of 0.45 eV, and consists of four bands, which is shown to be derived from the (again doubly-degenerate) e_{2u} HOMO's of an isolated coronene molecule.
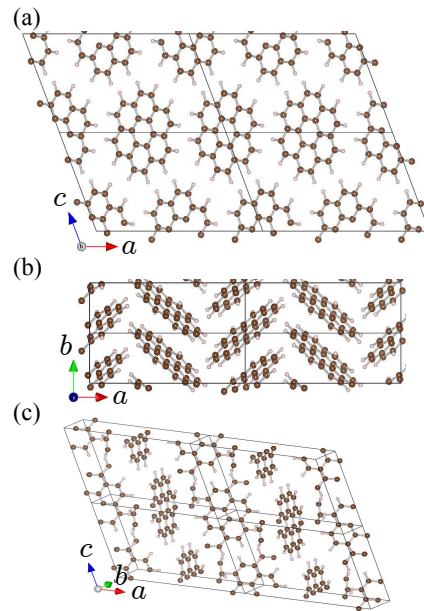

FIG. 1: (Color online) Crystal structure of undoped solid coronene viewed along (a) b axis, (b) c axis and (c) a bird's eye view. Solid lines delineate unit cells.

Downfolding — We have constructed an *ab initio* tight-binding model from the maximally localized WF's [11] of the four-fold conduction band. The two-fold degenerate e_{1g} LUMO's for an isolated molecule have b_{3g} and b_{2g} symmetries in the D_{2h} representation. Figure 3(a) displays the two WF's localized at each of the molecules. While the downfolded tight-binding band (not shown) accurately reproduces the DFT-LDA band structure, we can notice that the WF w_h is derived mainly from b_{3g} orbital while w_l from b_{2g}. The difference in the orbital energy between the two WF's is 18.2 meV, which is to be compared with 11.3 meV for solid picene. Figure 3(b,c) depicts the major transfer integrals in the downfolded tight-binding model, which exhibit the transfers along b axis much stronger than the other axes, in contrast to those in picene (see Fig. 3(c) in Ref.[8]), for which two transfers on $a - b$ plane are close to each other. The
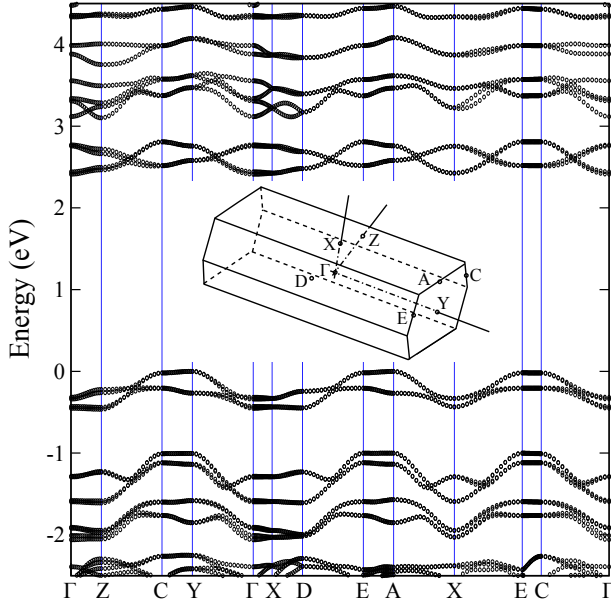
FIG. 2: (Color online) Calculated electronic band structure of the undoped crystalline coronene. The origin of the energy is set to be the valence band top. The inset depicts the Brillouin zone with Γ, Z, C, Y, X, D, E and A respectively corresponding to $(0,0,0)$, $(0,0,1/2)$, $(0,1/2,1/2)$, $(0,1/2,0)$, $(1/2,0,0)$, $(1/2,0,1/2)$, $(1/2,1/2,1/2)$ and $(1/2,1/2,0)$ in units of $(\mathbf{a}^*, \mathbf{b}^*, \mathbf{c}^*)$.
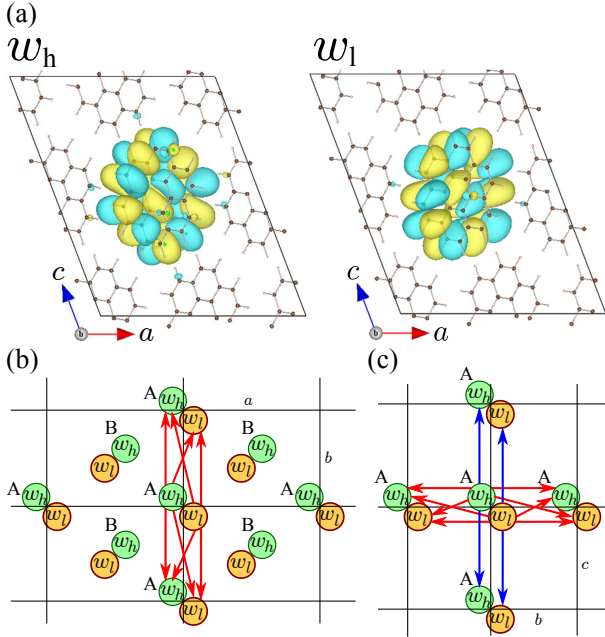

FIG. 3: (Color online) (a) displays maximally localized Wannier functions (right) w_l (w_h) with a lower-energy (higher-energy) constructed from the conduction bands of undoped solid coronene. Their transfer integrals t on the $a-b$ plane (b) and $b-c$ plane (c) are also shown, where the red (blue) arrows are for $|t| > 30$ meV ($10 < |t| < 30$ meV).

anisotropy of the transfers in coronene thus comes from the relative distances between the WF's.

Doped solid coronene — Let us finally discuss the doped coronene. If we naively adopt a rigid-band picture for a doping level of $x = 3$ for which superconductivity is observed, the Fermi surface (not shown) consists of multiple surfaces that comprise one-dimensional (planar) surfaces and a two-dimensional (cylindrical) one, along with a more three-dimensional one. However, since we have shown for the doped picene[8] that the rigid-band picture is broken in this material for two-fold reasons (i.e., a distorted herringbone structure upon doping along with a spilling of the molecular wave function over to potassium sites), we should have a look at the electronic structure of the coronene actually doped with K. Since the structure of the doped system has not been experimentally obtained, we have tried a structural optimization of K_3coronene. Since this in itself is an important but vast task, here we only show a candidate structure. We started from a plausible geometry with one potassium atom just above the molecule and two in the interstitial region. The initial coordinates of the six potassium atoms we adopted are $(1/2,0,0), (0,1/2,0), (\pm 1/3, 1/2, \pm 1/3)$ and $(\pm 5/6, 0, \pm 1/3)$, which preserve the monoclinic symmetry. Interestingly, the optimization, with the lattice parameters fixed at those for the pristine structure, resulted in a significant rearrangement of the herringbone structure with the monoclinic symmetry lowered, along with a strong deformation of each molecule, as seen in Figs. 4(a) and (b). The band structure of the K_3coronene is significantly more dispersive than the undoped one, where the LUMO-derived band group is fused with the upper band group, resulting in a much wider band group, as shown in Fig. 4(c). We can see that the resultant Fermi surface is an intriguing composite of one-dimensional surfaces (i.e., multiple pairs of planar surfaces) with different anisotropies. The doped picene also has a coexistence of multiple Fermi surfaces[8], but the doped coronene has topology of the surface different from those in doped picene, which comes from different (and more one-dimensional) tight-binding structure (Fig. 3(b,c)). The anisotropic, multiple Fermi surface should give a basis for examining superconductivity. In a phonon mechanism the problem becomes the coupling between the electrons on such a Fermi surface and the molecular phonons. The situation gives an interesting possibility for electron mechanisms as well, since the nesting between disconnected Fermi surfaces can give rise to a unique opportunity for an electron mechanism, especially in multiband cases.[23] For an accurate description of the structure more elaborate and exhaustive structural optimizations will be needed, since the large degrees of freedom on the dopant positions will render the energy surface many local minima. Such a systematic examination is, however, beyond the scope of the present work, and will be reported in future.

Finally, a few words about the "aromaticity" of

molecules. Its simplest definition is in terms of the "Clar sextets" (resonating benzene rings)[24] on a given molecular structure. When a molecule is fully benzenoid (where the sextets exhaust all the double bonds) the wave function tends to be localized on the sextets. In this picture picene is non-fully-benzenoid, while coronene, also non-fully-benzenoid, has multiple Clar structures.[21] The relation of these quantum chemical properties with band structures is another of interesting future problems.

In summary, we have studied the electronic structure of solid coronene by means of first-principles calculation. The conduction band is found to comprise four bands, which basically originate from the lowest two unoccupied molecular orbitals (doubly-degenerate, reflecting the molecular symmetry) in an isolated molecule, but the bands are entangled. The maximally localized WF's are used to derive a downfolded tight-binding Hamiltonian, where the major transfer integrals are found to significantly differ from those in solid picene. The Fermi surface for a candidate of the structure of $K_x$coronene with $x = 3$, for which superconductivity is found, comprises multiple sheets, as in doped picene but with different topology of the surface. Their relevance to superconductivity is an interesting future problem.
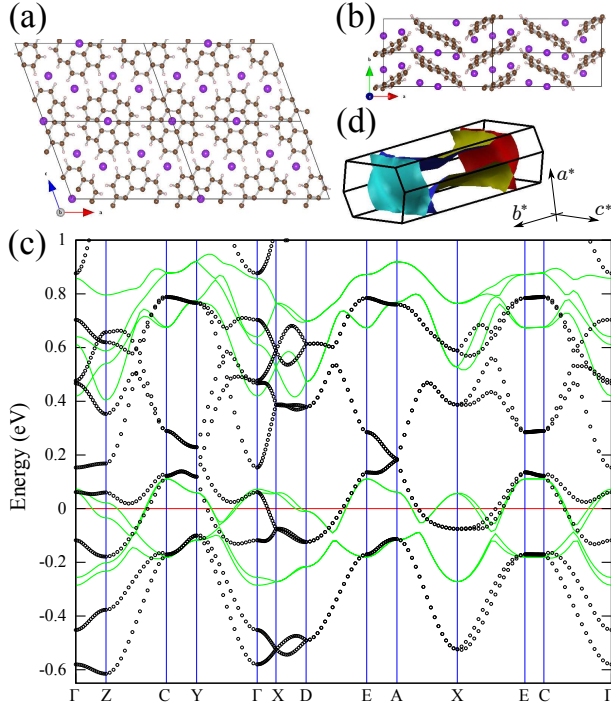
FIG. 4: (Color online) Crystal structure of K_3coronene viewed along (a) b or (b) c axis. Larger balls represent K atoms. (c) shows electronic band structures of the K_3coronene (circles) and undoped coronene (curves). The origin of energy for the K_3coronene is set to its Fermi level while that for undoped coronene set for $x = 3$ in a rigid-band shift for comparison. The Fermi surface for the K_3coronene is displayed in (d).

[1] R. Mitsuhashi, Y. Suzuki, Y, Yamanari, H. Mitamura, T. Kambe, N. Ikeda, H. Okamoto, A. Fujiwara, M. Yamaji, N. Kawasaki, Y. Maniwa, and Y. Kubozono, Nature **464**, 76 (2010).

[2] N. B. Hannay, T. H. Geballe, B. T. Matthias, K. Andres, P. Schmidt, and D. MacNair, Phys. Rev. Lett. **14**, 225 (1965).

[3] T. E. Weller, M. Ellerby, S. S. Saxena, R. P. Smith and N. T. Skipper, Nature Phys. **1**, 39 (2005); N. Emery, C. Hérold, M. d'Astuto, V. Garcia, Ch. Bellin, J. F. Marêché, P. Lagrange and G. Loupias, Phys. Rev. Lett. **95**, 087003 (2005).

[4] A. F. Hebard, M. J. Rosseinsky, R. C. Haddon, D. W. Murphy, S. H. Glarum, T. T. M. Palstra, A. P. Ramirez and A. R. Kortan, Nature **350**, 600 (1991).

[5] K. Tanigaki, T. W. Ebbesen, S. Saito, J. Mizuki, J. S. Tsai, Y. Kubo and S. Kuroshima, Nature **352**, 222 (1991).

[6] T. T. M. Palstra, O. Zhou, Y. Iwasa, P. E. Sulewski, R. M. Fleming and B. R. Zegarski, Solid State Commun. **93**, 327 (1995).

[7] E. A. Ekimov, V. A. Sidorov, E. D. Bauer, N. N. Melfnik, N. J. Curro, J. D. Thompson, and S. M. Stishov, Nature **428**, 542 (2004).

[8] T. Kosugi, T. Miyake, S. Ishibashi, R. Arita and H. Aoki, J. Phys. Soc. Jpn. **79**, 044705 (2010).

[9] Y. Kubozono, M. Mitamura, X. Lee, X. He, Y. Yamanari, Y. Takahashi, Y. Suzuki, Y. Kaji, R. Eguchi, K. Akaike, T. Kambe, H. Okamoto, A. Fujiwara, T. Kato, T. Kosugi, and H. Aoki, submitted.

[10] X. F. Wang, R. H. Liu, Z. Gui, Y. L. Xie, Y. J . Yan, J. J. Ying, X. G. Luo and X. H. Chen, arXiv:1102.4075v1 (unpublished) have reported that $K_x$phenanthrene also exhibits superconductivity with $T_c \simeq 5$ K.

[11] N. Marzari and D. Vanderbilt, Phys. Rev. B **56**, 12847 (1997); I. Souza, N. Marzari and D. Vanderbilt, Phys. Rev. B **65**, 035109 (2001).

[12] See, e.g., K. Kuroki, J. Phys. Soc. Jpn. **75**, 051013 (2006).

[13] G. Giovannetti and M. Capone, Phys. Rev. B **83**, 134508 (2011).

[14] M. Kim, B. I. Min, G. Lee, H. J. Kwon, Y. M. Rhee and J. H. Shim, arXiv:1011.2712v1 (unpublished).

[15] T. Kato and T. Yamabe, J. Chem. Phys. **115**, 8592 (2001); T. Kato, K. Yoshizawa and K. Hirao, J. Chem. Phys. **116**, 3420 (2002); T. Kato and T. Yamabe, Chem. Phys. **325**, 437 (2006).

[16] A. Subedi and L. Boeri, arXiv:1103.4020v1 (unpublished).

[17] D. M. Ceperley and B. J. Alder, Phys. Rev. Lett. **45**, 566 (1980); J. P. Perdew and A. Zunger, Phys. Rev. B **23**, 5048 (1981).

[18] P. E. Blöchl, Phys. Rev. B **50**, 17953 (1994); G. Kresse and D. Joubert, Phys. Rev. B **59**, 1758 (1999).

[19] http://www.qmas.jp/

[20] T. Echigo, M. Kimata and T. Maruoka, American Mineralogist **92**, 1262 (2007).

[21] T. M. Krygowski, M. Cyrański, A. Ciesielski, B. Świrska and P. Leszczyński, J. Chem. Inf. Comput. Sci. **36**, 1135 (1996).

[22] F. Roth, M. Gatti, P. Cudazzo, M. Grobosch, B. Mahns, B. Büchner, A. Rubio and M. Knupfer, New J. Phys. **12**, 103036 (2010).

[23] H. Aoki, Physica B **404**, 700 (2009).

[24] E. Clar, Polycyclic Hydrocarbons, Academic Press, London, 1964